Defect structure of NH4 + βalumina studied by NMR

H. Arribart, H. Carlos, and B. Sapoval

Citation: The Journal of Chemical Physics **77**, 2336 (1982); doi: 10.1063/1.444153
View online: http://dx.doi.org/10.1063/1.444153
View Table of Contents: http://scitation.aip.org/content/aip/journal/jcp/77/5?ver=pdfcov
Published by the AIP Publishing

Defect structure of NH_4^+ β-alumina studied by NMR

H. Arribart, H. Carlos, and B. Sapoval

Laboratoire de Physique de la Matière Condensée,[a] *Ecole Polytechnique, 91128 Palaiseau, France*
(Received 17 March 1982; accepted 3 May 1982)

The behavior of proton NMR absorption spectra in nonstoichiometric NH_4^+ β-alumina single crystal has been studied between 90 and 230 K, below the onset of translational motion narrowing. Below 140 K the signal is the superposition of a broad line due to motionless NH_4^+ ions in mid-oxygen sites and of a narrow line due to rapidly rotating ions in Beevers–Ross sites. Above 160 K all the ions rotate and both lines merge into a single line. A detailed quantitative analysis of the second moments of these lines enables us to show that the defect related to the nonstoichiometry is made of two pairs of NH_4^+ ions in displaced mid-oxygen sites. Perfect agreement between theory and experiment is found if one takes into account small displacements of the Beevers–Ross ions from their high symmetry sites, the size and the shape of the NH_4^+ ions, and the specific orientations of the displaced Beevers–Ross and mid-oxygen ions. This study shows in particular that the population of anti-Beevers–Ross sites is vanishingly small at the temperatures where the translational motion is slow, showing that there is a close link between ionic conductivity and anti-Beevers–Ross occupancy.

I. INTRODUCTION

It is obvious that a comprehensive understanding of the conduction mechanism in nonstoichiometric fast ion conductors requires the knowledge of the structure of the defect related to this nonstoichiometry. This is the case of the β-aluminas[1] for which Wolf[2] recently proposed a detailed microscopic model for the conductivity, based on the idea that the compensation of excess cations is due to the presence of O^{2-} ions sitting in mid-oxygen (mO) positions.[3] At low temperature, the excess cations are trapped near these extra O^{2-} and they are progressively released as the temperature is increased, giving interstitialcy pairs moving in a stoichiometric medium between these defects. The idea of a charge transport caused by hopping of an interstitialcy pair defect on the honeycomb network was introduced by Whittingham and Huggins[4] and was supported by the theoretical calculation[5] of the potential barrier for such a movement in a stoichiometric material. Although a number of experiments have been performed on these systems, only a few can be critically examined in the light of these ideas.[2] Most experiments give macroscopic averages which are only weakly dependent on the detail of the defect structure.

We show in this work that in this respect nuclear magnetic resonance can be a very powerful tool especially in protonic conductors where the interaction between protons is the magnetic dipole–dipole interaction which depends only on the geometry of the system. This interaction is very sensitive to the distance between spins; e.g., a pair of nearest mO ions contribute to the interionic second moment of the resonance line as much as $2^6 = 64$ pairs of ions in Beevers–Ross (BR) sites. A comprehensive quantitative analysis of the second moments shows that the defect related to nonstoichiometry is made of two pairs of ions in displaced mO positions as shown in Fig. 3(a). In particular, an appreciable population of anti-Beevers–Ross (aBR) sites is not allowed below 230 K. Only when the translational diffusion occurs, the aBR occupancy may become appreciable.

Even very fine details of the geometry of the defect play a role in the value of the proton second moment: slightly displaced positions of the center of the cations from the high symmetry sites and orientation of the NH_4^+ tetrahedra with respect to the crystal axis. By taking all these factors into account, a perfect agreement between theory and experiment is arrived at. This gives strong support to the proposed structure of the defect.

We describe experimental results in Sec. II. We next proceed in two steps, In Sec. III, we consider the NH_4^+ ions as point ions with the four protons placed at the center of gravity. The second moment analysis then permits us to show that the defect related to nonstoichiometry is made of two pairs of NH_4^+ ions in displaced mO sites (dmO) as shown in Fig. 3(a). In Sec. IV, we propose a complete geometrical description of the defect taking into account slight displacements of BR ions evidenced from the x-ray data[6] and realistic well-defined orientations for the NH_4^+ ions. We consider the two different orientations which have been proposed for BR ions, one by Colomban *et al.*[6] and Bates *et al.*[7] and the other by Gourier and Sapoval.[8]

II. EXPERIMENTAL RESULTS

Several NMR studies of NH_4^+ β-alumina have already been published.[8–10] Although some reported results differ, possibly as a result of differences between samples, the following common features were found.

At very low temperatures, the study of spin isomerism[11] has shown that there were two kinds of NH_4^+ ions, not a surprising result considering the nonstoichiometry of the material. The ions in BR sites undergo rapid rotational tunneling, whereas the other ions (probably in mO sites) are more strongly bonded to the lattice and are not tunneling.[8]

Between 90 and 230 K, a single line has been reported which was attributed in Ref. 8 to ions rotating around specific axis. This line was attributed in Ref. 9 to completely rotating ions behaving as in the stoichiometric compound. We will see that these results are incom-

[a] Groupe de Recherche No. 38 du Centre National de la Recherche Scientifique.

 0021-9606/82/172336-08$02.10

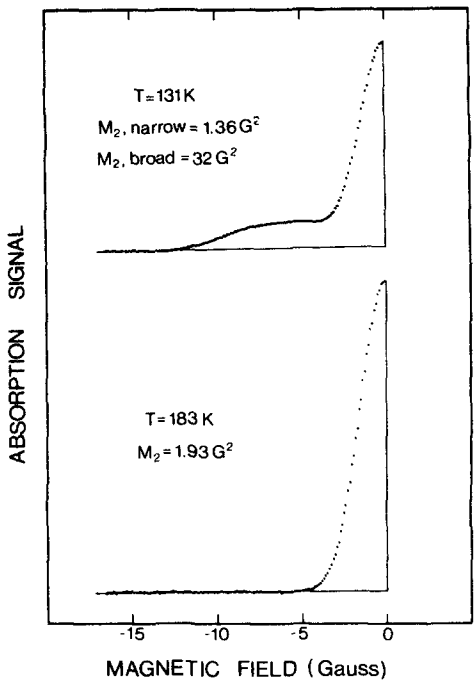

FIG. 1. Proton NMR absorption of $11Al_2O_3$. $1.3(NH_4)_2O$ single crystal at 131 and 183 K with H_0 parallel to the crystal c-axis. The figure shows the integrated experimental signal obtained at $H_0 = 1.88$ kG with peak-to-peak rf field of 24 mG and peak-to-peak modulation of 2 G. The sweep rate was 20 G per h. Only a half of the spectrum is shown.

plete and that the proposed interpretations must be reconsidered.

At still higher temperatures complete motion narrowing due to translational diffusion occurs.[8-10] This regime shows low dimensionality effects which will be studied in detail in a forthcoming paper.[12]

The first aim of the research reported here was to search for the signal of mO ions in the intermediate temperature range. The fact that they do not tunnel at low temperature indicates that their rotation is strongly hindered. This fact is sustained by the values of the potential barriers for rotation calculated by Bates *et al.*[7] Then, these ions should give the broad line of static NH_4^+[13] in contradiction to the BR ions which experience a weak energy barrier for rotation. The BR ions undergo tunneling at 4.2 K and rapid thermally activated reorientations at 90 K leading to the already reported narrow line, observed below 230 K.

And indeed, a very careful set of experiments allowed us to observe a very broad line as well as a narrow line (see Fig. 1). Such a signal was not reported in Ref. 8 since the broad component of the signal is very weak. It is of the same magnitude as the small signal of the protons of the Varian probe head.

In the present study, NMR spectra were obtained by conventional wide-line techniques on a single crystal of NH_4^+ β-alumina. The material was obtained by chemical exchange from a crystal of Na^+ β-alumina of composition $11Al_2O_3$. $(1+x)Na_2O$ with $x = 0.3$. The crystal was grown by the Czochralsky technique. A sodium neutron activation analysis of the exchanged crystal indicates an exchange rate of 98%. We have been able to obtain the signals of Fig. 1 by optimizing the signal-to-noise ratio using very slow passages. The sample signal was obtained by substracting the signal of the empty probe head from the signal of the probe head with the crystal. This difference was digitally integrated. The narrow line has a linewidth between the peaks of the absorption derivative of 2.8 ± 0.1 G as reported in Ref. 8. The broad line has a width of 20 G, a value typical of a static NH_4^+ spectrum.[13]

The existence of two lines is evidence of the existence of two types of ions and cells in the nonstoichiometric compound. We recall that at weak rf fields, the area under an NMR absorption line is proportional to the number of nuclei in resonance. Here, the ratio of the area under the narrow line to the area under the broad line is measured to be 1.05 ± 0.10. This can be compared to the ratio ρ of the number of ions in BR sites (in singly occupied cells) to the number of ions in mO sites (in doubly occupied cells). With the composition $x = 0.3$, ρ is equal to $0.7/0.6 = 1.17$. The agreement between these two values demonstrates that the nonstoichiometry is achieved by double occupation of some of the unit cells. The occurrence of a nonstoichiometry due to the triple occupancy of unit cells by excess cations, as in Mg^{2+} substituted β-alumina,[14] which should give $\rho = 0.85/0.45 = 1.89$ is not possible.

This same spectrum is observed between 90 and 140 K. Above 140 K, the broad line narrows and the two lines progressively merge into a single line of nearly Gaussian shape with a width between the peaks of the absorption derivative of 3.0 ± 0.1 G. This narrowing is attributed to the onset of rotation of mO ions. We have not studied in detail the behavior of the spectrum in the intermediate range 140–180 K because the experimental procedure is very tedious. The single narrow line is observed to have a constant linewidth from 180 to 230 K.

We have measured the second moments of all absorption line components.[14] For $T < 140$ K, the second moments of the narrow line "alone" and of the broad line "alone" are, respectively,

$$M_N = 1.36 \pm 0.10 \text{ G}^2 ,$$

$$M_B = 32 \pm 2 \text{ G}^2 .$$

The above value of M_N is obtained assuming that the broad line is flat at the center of the spectrum although the spectrum of a static NH_4^+ ion has a small narrow component.[16] We have calculated that the largest possible error due to this approximation is -0.15 G^2. The value $M_N = 1.36 \pm 0.10$ G^2 must then be considered as a maximum value. The total second moment is measured to be $M_T = 15 \pm 2$ G^2, in accordance with the expression

$$M_T = \frac{n_N M_N + n_B M_B}{n_N + n_B} ,$$

where n_N and n_B are the numbers of spins contributing to the narrow and broad lines.

For $T > 180$ K, the second moment of the single line is

$M_S = 1.93 \pm 0.10\ G^2$.

These values differ from the second moment value of $7 \pm 2\ G^2$ reported in Ref. 8 for the "single" line. In fact, this value was measured at 160 K, i.e., in the temperature range where we show here that the total second moment progressively decreases from 15 G^2 to 1.93 G^2. Since the shape of the narrow line (the only observed signal at that time) is nearly constant, this value of the second moment was believed to be valid in the whole range 90–230 K.

III. SECOND MOMENT ANALYSIS

The theory of second moments of NMR lines is well established and verified.[17] The broadening interaction is the classical magnetic dipole–dipole interaction which depends only on the geometrical arrangement of the nuclear spins. In general, this is well understood, but in our case, it will be important to realize that protons pertaining to nonrotating ions which have a very broad spectrum have to be considered as "unlike" spins for protons pertaining to rotating ions. We will show that this permits us to explain the broadening of the narrow line between 140 and 180 K. The purpose of our analysis is then to find a defect structure which can explain the measured second moments. We will show that only defects made of two pairs of NH_4^+ ions in displaced mid-oxygen (dmO) positions are compatible with the experimental results.

The spin system in NH_4^+ β-alumina is composed of three different nuclear species: ^1H, ^{27}Al, and ^{14}N. Considering the proton resonance, one has to distinguish between intraionic and interionic interactions, the latter being one order of magnitude smaller. The spectrum of one isolated static NH_4^+ ion is made up of several discrete lines spread over 20 G, due to intraionic ^1H–^1H and ^1H–^{14}N dipole–dipole interactions. The spectrum of a rapidly rotating isolated NH_4^+ ion is a single line. In a solid, these spectra are broadened by interionic interactions between protons and between protons and ^{27}Al nuclei (the interionic ^1H–^{14}N interaction is negligible). We will be concerned in the following by the two narrow lines observed between 90 and 130 K and between 180 a and 230 K, for which the rotation averages to zero the intraionic interaction. For this reason, only interionic broadening is considered.

The second moment due to the interaction between like spins labeled j and k is[17]:

$$M_L = \tfrac{3}{4}\gamma_I^4\hbar^2 \frac{I(I+1)}{N} \sum_{j\neq k} \frac{(1-3\cos^2\theta_{jk})^2}{r_{jk}^6} , \tag{1}$$

where r_{jk} is the distance between spins j and k, θ_{jk}, the angle between r_{jk} and the external field and N the total number of observed spins.

The expressions for the second moment due to the interaction with unlike spins labeled l is[17]:

$$M_U = \tfrac{1}{3}\gamma_I^2\gamma_l^2\hbar^2 \frac{S_l(S_l+1)}{N} \sum_{j,l} \frac{(1-3\cos^2\theta_{jl})^2}{r_{jl}^6} . \tag{2}$$

In NH_4^+ β-alumina, the unlike spins are first the ^{27}Al nuclei, but one must emphasize that at low temperature, the protons belonging to nonrotating ions have also to be considered as unlike spins for the protons belonging to rotating ions that we observe in the narrow line. The reason is that in the theory of dipolar broadening, one has to be careful to remove from the dipolar Hamiltonian all the terms which do not conserve energy.[17] This has to be made for flip-flop terms between spins of different nuclear species, but it has also to be made here when considering the flip-flop interaction between the spins of static and rotating ions. In the temperature regime where all ions are rotating, all protons must be considered as like spins.

We can now calculate the second moment of the narrow line in the two temperature regimes for H_0 parallel to the crystal c axis (an angular dependence has been observed and will be reported elsewhere[12]). We write the second moment as the sum of three terms:

$$M_{N,S} = m_{H,like} + m_{H,unlike} + m_{Al} \tag{3}$$

with

$$m_{H,like} = \frac{9}{16} \frac{\gamma_H^4\hbar^2}{N} \Sigma^1 , \tag{4}$$

$$m_{H,unlike} = \frac{1+y}{4} \frac{\gamma_H^4\hbar^2}{N} \Sigma^2 , \tag{5}$$

and

$$m_{Al} = \frac{35}{12} \frac{\gamma_H^2\gamma_{Al}^2\hbar^2}{N} \Sigma^3 . \tag{6}$$

Here, Σ^1 is the sum of r_{jk}^{-6} over all protons j and k belonging to different rotating NH_4^+, Σ^2 is the sum of r_{jl}^{-6} over all protons j belonging to rotating NH_4^+ ions and all protons l belonging to static NH_4^+ ions and Σ^3 is the sum of $(1-3\cos^2\theta_{j,l'})^2\, r_{jl'}^{-6}$ over all protons j belonging to rotating NH_4^+ ions and all ^{27}Al nuclei l' in the spinel blocks. The value of Σ^2 will be zero in the high temperature range since all ions are rotating. The enhancement factor $1+y$ in Eq. (5) takes into account the partial like character of the static ammonium-rotating ammonium interaction due to the partial overlap of the broad and narrow components of the absorption spectrum. A rough estimation of y is $\delta H_N/\delta H_B$, where δH_N and δH_B are the linewidths of the narrow and broad components, respectively. We have taken in the following $y = 0.15$. Since we are dealing with a disordered material, it is not *a priori* possible in Eqs. (4)–(6) to write $\sum_{j\neq k} = N\sum_k$ because not all protons j have the same neighbors.

At this stage, it is necessary to have a picture of the possible geometric arrangements of ammonium ions which are compatible with the cation content of the conduction plane. Figure 2 shows two *a priori* possible arrangements of cations around the charge compensation defect, assumed to be an interstitial O^{2-} ion in mO position. Figure 2(a) shows the defect proposed in Ref. 3 which is made of two pairs of ions in mO positions. In the case of NH_4^+ β-alumina, a partial occupation of aBR sites has been evoked[6] so that we must also consider the defect shown in Fig. 2(b) which is made of one pair of mO ions plus one ion in aBR position. We see that, in each case, the defect spreads on a number of about 10 unit cells. The concentration of defect O^{2-}

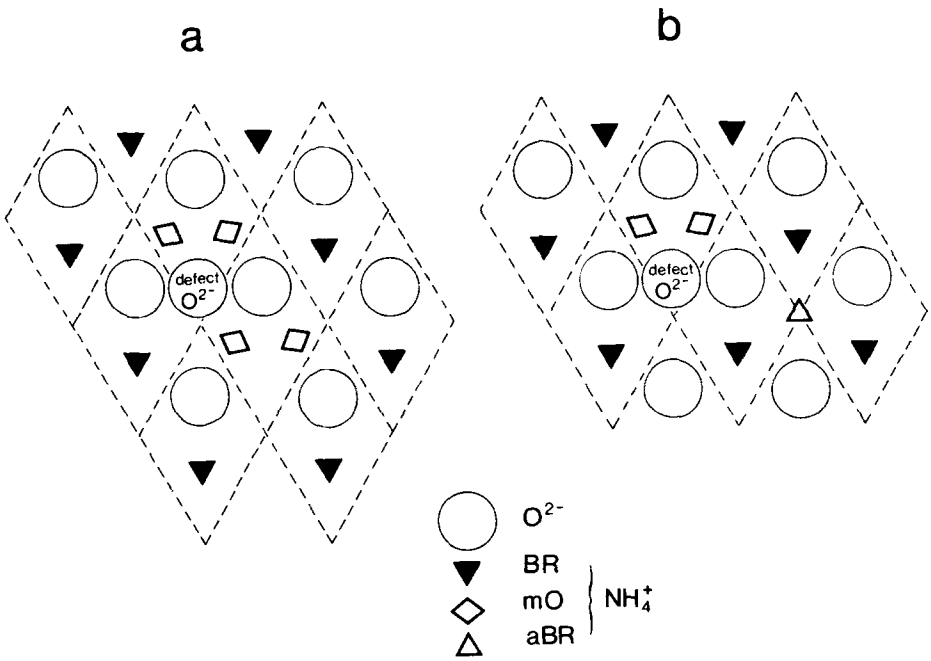

FIG. 2. Possible defect structure with point ions in the true high symmetry positions. The charge compensating interstitial O^{2-} is situated in mO position. (a) Four cations are situated in the nearest possible mO positions. (b) One cation occupies the nearest possible aBR position.

being 0.15 per cell for the composition $x = 0.3$, this suggests that each ammonium ion is disturbed by at least one defect: the probability for NH_4^+ ion in a BR site to be surrounded only by NH_4^+ ions in BR sites, as in the stoichiometric compound, is negligible. We must then consider the ions individually in evaluating the various sums. For that, we use the simplifying hypothesis that the nonstoichiometric arrangement of the ions is made of a pavement of either of the defects shown in Fig. 2.

In case 2(a), the number of protons in BR, mO, and aBR sites is, respectively,

$$N_{BR} = 4 \times 0.7 \times n_c ,$$

$$N_{mO} = 4 \times 0.6 \times n_c ,$$

$$N_{aBR} = 0 ,$$

where n_c is the number of unit cells. The factor 4 indicates that each NH_4^+ ion contains four protons which

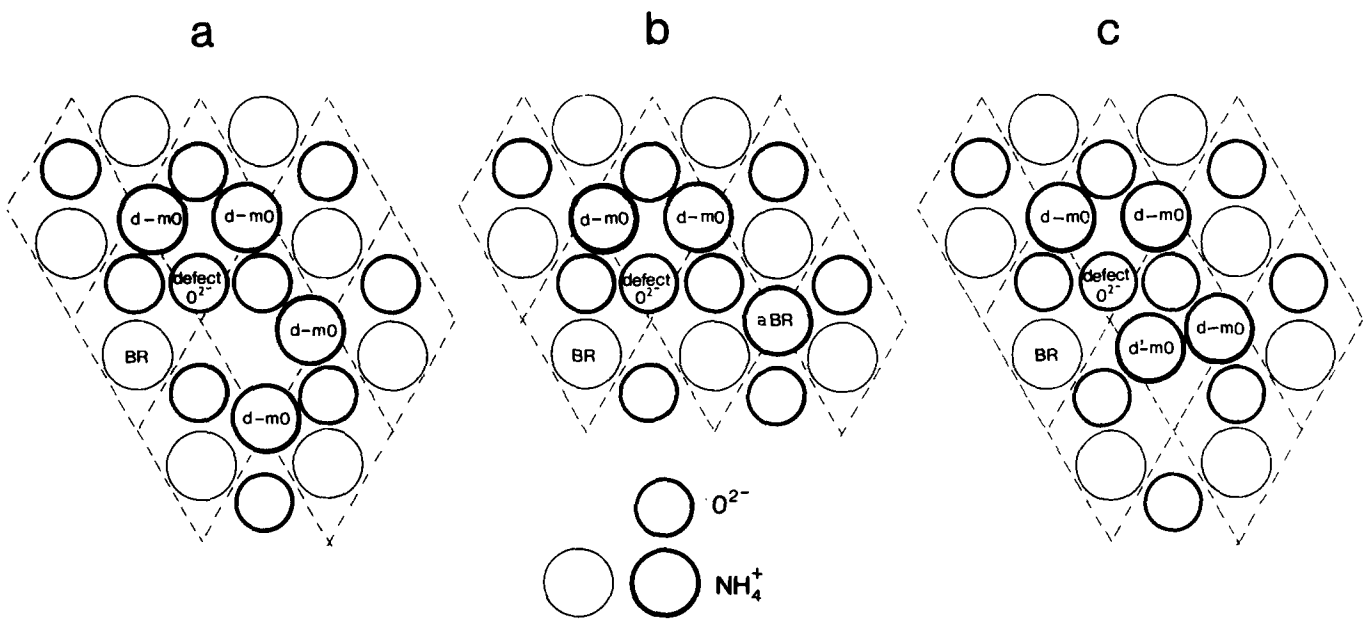

FIG. 3. Possible defect structures with "relaxed" mO ions. The size of the circles approximately reproduces the ionic radii. Ammonium ions in "normal" BR sites are represented by thin circles. Ammonium ions in "defect" sites are represented by strong circles. (a) Two pairs of mO ions displaced from mO towards aBR. (b) The mO ions are displaced from mO towards aBR positions, one ion sitting in aBR. (c) Three mO ions displaced from mO towards aBR plus one ion (d'mO) displaced from mO towards BR. Only cases (a) and (b) are compatible with x-ray studies.

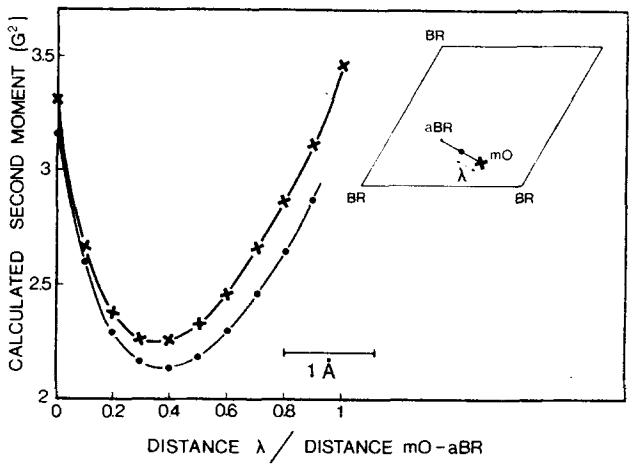

FIG. 4. Variation of the calculated second moment M_S as a function of the distance between the dmO ion and the true mO site for defect 3(a). Crosses give the second moment values when the BR ions occupy the high-symmetry crystallographic sites as shown in Fig. 3(a). Full circles give the second moment values when the BR ions are displaced by 0.13 Å towards mO sites as shown in Fig. 5.

are supposed to sit at the center of the ion.

In case 2(b), the number of protons is

$$N_{BR} = 4 \times 0.85 \times n_c ,$$

$$N_{mO} = 4 \times 0.3 \times n_c ,$$

$$N_{aBR} = 4 \times 0.15 \times n_c .$$

At low temperatures, we propose that only BR ions rotate, so that $N = N_{BR}$, while, in the high temperature regime, $N = N_{BR} + N_{mO} + N_{aBR} = 5.2\, n_c$.

For low temperatures, we can then write

$$\Sigma^1 = 4N_{BR}\bar{\Sigma}^1_{BR},$$

$$\Sigma^2 = 4N_{BR}\bar{\Sigma}^2_{BR} ,$$

$$\Sigma^3 = 4N_{BR}\bar{\Sigma}^3_{BR} ,$$

where $\bar{\Sigma}^1_{BR}$, $\bar{\Sigma}^2_{BR}$, and $\bar{\Sigma}^3_{BR}$ are the averages over the different environments for a BR ion found in Fig. 2. The factor 4 stands for four protons assumed to be at the center of each neighboring ion. With this notation, $\bar{\Sigma}$ is the average of the sum of r^{-6}. For example, in a stoichiometric compound, neglecting second neighbors, we would have $\bar{\Sigma}^1_{BR} = 6a^{-6}$.

At high temperatures, it holds

$$\Sigma^1 = 4N_{BR}\bar{\Sigma}^1_{BR} + 4N_{mO}\bar{\Sigma}^1_{mO} + 4N_{aBR}\bar{\Sigma}^1_{aBR} ,$$

$$\Sigma^2 = 0 ,$$

$$\Sigma^3 = 4N_{BR}\bar{\Sigma}^3_{BR} + 4N_{mO}\bar{\Sigma}^3_{mO} + 4N_{aBR}\bar{\Sigma}^3_{aBR} ,$$

where $\bar{\Sigma}^1_{mO}$, $\bar{\Sigma}^1_{aBR}$, $\bar{\Sigma}^3_{mO}$, and $\bar{\Sigma}^3_{aBR}$ are the averages over the different ionic environments for a given site found in Fig. 2.

The results of the computation are presented in Tables I and II. They have been obtained with the values $a = 5.59$ Å and $c = 22.81$ Å for the crystal parameters.[6] The summation has been performed up to a 10 Å distance. For comparison, we give the calculated second moment of the stoichiometric compound ($x = 0$), where all the ions sit in the BR sites and all protons are alike at all temperatures. We give also the values calculated for a fictitious "mean" crystal of composition $x = 0.3$. In this mean crystal, the conduction plane is assumed to be hexagonal as in the stoichiometric material, but with a lattice parameter scaled to keep the density of NH_4^+ ions the same as in the real material.

One sees that the values obtained for defects 2(a) and 2(b) are much larger than the experimental values. Even if we take care of the possible corrections due to the true geometry of the ion [this is made in Sec. IV for the defect 3(a)], one finds that the experiment is not compatible with the existence of defect 2(a) or defect 2(b).

So far we have considered only defects made of ions in the classical high symmetry positions. This is unrealistic for mO pairs because of the size of the NH_4^+ cation. We therefore consider now "relaxed" defects in which the mO ions sit, in fact, on mO–aBR or mO–BR lines. For steric and electrostatic considerations, only three defects are conceivable. They are shown in Fig. 3. In case 3(a), the defect is made of two pairs of ions between mO and aBR sites. In case 3(b), the defect consists of one ion in a true aBR site plus a pair of ions on mO–aBR lines, and in case 3(c) three mO ions are displaced towards the aBR position and one mO ion is displaced towards the BR position. We then have to find among these defects those which are compatible with the x-ray results of Colomban *et al.*[6] and with our NMR results. Since the evidence from x-ray that the mO–BR line is free from electronic density excludes defect 3(c), only second moment calculations for defects 3(a) and 3(b) have been performed.

One should emphasize that, due to the r^{-6} dependence, the second moment values vary rapidly with the distance. This is illustrated in Fig. 4, where the variation of M_S in case 3(a) is drawn as a function of the displacement from the true mO position. The values given

TABLE I. Theoretical values of the second moment $M_N(G^2)$ in the low temperature regime [see expression (3)].

	Stoichiometric material	Mean crystal	Figure 2(a) defect	Figure 2(b) defect	Figure 3(a) defect	Figure 3(b) defect
$m_{H,like}$	0.38	0.80	0.30	0.33	0.30	0.33
$m_{H,unlike}$	0	0	0.14	0.45	0.26	0.56
m_{Al}	0.92	0.92	0.92	0.92	0.92	0.92
$M_{N,th}$	1.30	1.72	1.36	1.70	1.48	1.81

TABLE II. Theoretical values of the second moment $M_S(G^2)$ in the high temperature regime [see expression (3)].

	Stoichiometric material	Mean crystal	Figure 2(a) defect	Figure 2(b) defect	Figure 3(a) defect	Figure 3(b) defect
$m_{H,like}$	0.38	0.80	2.30	2.34	1.28	1.74
$m_{H,unlike}$	0	0	0	0	0	0
m_{Al}	0.92	0.92	1.02	0.98	0.99	0.94
$M_{S,th}$	1.30	1.72	3.32	3.32	2.27	2.68

in Tables I and II for the defects 3(a) and 3(b) correspond to the minimum of this variation. The computed values are significantly larger than the experimental values even if one considers the ions sitting at the position which gives the smallest second moment. This is especially true for defect 3(b) for which both M_N and M_S are incompatible with the experiment. We have considered also the possible influence of the so-called Frenkel defect in which two Al^{3+} ions are situated above and below the interstitial defect O^{2-} ion[3], but we have found that this has a negligible contribution in all cases. We believe that the difference between experiment and theory is sufficient to exclude defect 3(b). Therefore, we choose the defect 3(a) as the real defect. In this case, $M_{N,th} = 1.48\ G^2$ is comparable with $M_{N,expt} = 1.36 \pm 0.10\ G^2$ and $M_{S,th} = 2.27\ G^2$ with $M_{S,expt} = 1.93 \pm 0.10\ G^2$.

One could consider that this is a sufficient evidence for the existence of defect 3(a). However, since the Van Vleck theory of second moments due to dipole interaction is very accurate, we believe that the difference of $0.34\ G^2$ between the calculated and experimental values of M_S is significant. This difference has to be explained. In the next section, it is shown that it can be indeed quantitatively explained if one considers all the details of the geometry of the ions in their environment.

IV. EXACT GEOMETRY OF THE DEFECT

The next two refinements that are considered are first, the effect of the slight off-centering of the BR ions found in the x-ray studies[6] and second, the effect of the finite size of the NH_4^+ ion.

We first examine the effect of the 0.13 Å displacement of the NH_4^+ BR ions towards mO found in the x-ray studies. The displaced N atom is found statistically distributed in the three BR–mO directions.[6] Knowing the approximate defect structure 3(a), it is now possible to guess the true direction of the displacement of each of the NH_4^+ BR ions participating to the defect. We assume that the off-centering of the BR ions is the consequence of a mechanical relaxation due to an electrostatic repulsion with excess mO ions. This gives us a unique choice illustrated in Fig. 5 for the position of the center of each BR ion. From then, it is possible to calculate again the second moment as a function of the displacement of the mO ions. The result is shown in Fig. 4. The position of the minimum is only slightly changed, but the high temperature second moment value M_S at the minimum drops by $0.12\ G^2$. This variation comes from the proton–proton contribution mainly, the effect of the displacement on the ^1H–^{27}Al contribution being negligible.

So far, the four protons of the NH_4^+ ion were assumed to be located at the center of the ion. The ammonium ion is a tetrahedron with a N–H distance of 1 Å and with well-defined orientations even while rapidly reorientating. Then, if one considers a pair of neighboring NH_4^+ ions, the $4 \times 4 = 16$ proton–proton interactions should not be taken as equal. There are two cases: if the ions are static, one must take the sum of the 16 proton–proton pair contributions to the second moment

$$\sum_{i,j=1,2,3,4} \frac{(1-3\cos^2\theta_{ij})^2}{d_{ij}^6} \quad . \tag{7}$$

This quantity is larger than its approximate value 16 d^{-6}, where d is the N–N distance. Whenever the ions are rapidly reorientating, the dipole–dipole interaction must be averaged.[17] In that case, the above expression should be replaced by

$$\frac{1}{16}\left(\sum_{i,j=1,2,3,4} \frac{1-3\cos^2\theta_{ij}}{d_{ij}^3}\right)^2 \quad . \tag{8}$$

This value can be smaller or greater than 16 d^{-6} depending on the relative orientations of the two tetrahedra.

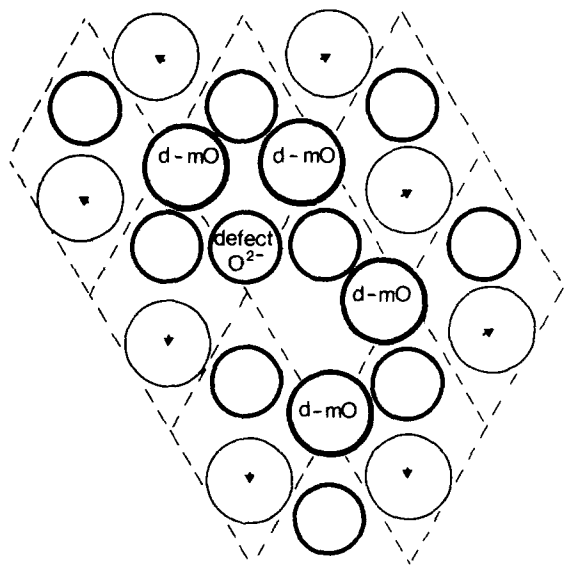

FIG. 5. Effect of mechanical relaxation of the BR ions in defect 3(a). The arrows represent the displacement of the center of the ions from the ideal BR sites towards mO sites.

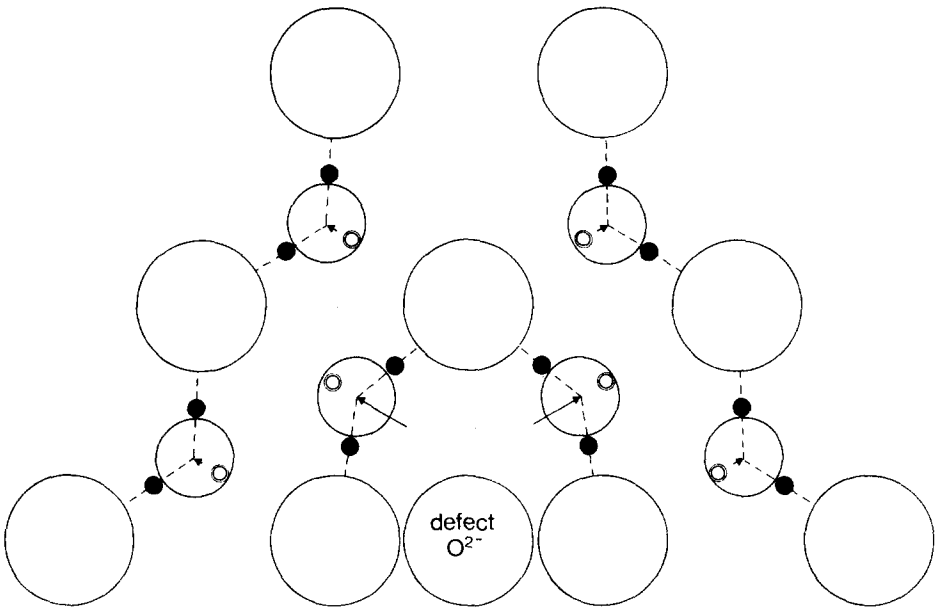

FIG. 6. Enlargement of the upper part of Fig. 5 to show the exact positions of the protons. All ions are taken in the Colomban *et al.* orientation with two protons in the conduction plane (full small circles) for hydrogen bonding with the nearest O(5) oxygens. Open small circles are the projection of the two out-of-plane protons. Large circles represent O(5) atoms. Long arrows represent the displacements of the center of the mO ions from mO towards aBR. Short arrows represent the displacements of the center of the BR ions from BR towards mO.

The magnitude of this effect can be large. For example, with a N–N distance of 4 Å, this sum can vary by a factor of 2 between specific orientations. A similar calculation must be made for the $^1H-^{27}Al$ interaction. In that case, the correct expression is

$$\left(\sum_{i=1,2,3,4} \frac{1-3\cos^2\theta_i}{d_i^3}\right)^2 \tag{9}$$

instead of $4d^{-6}(1-3\cos^2\theta)^2$. The value of the sums (8) and (9) depends on the relative orientations of the stable positions of the NH_4^+ ions and of their orientation with respect to the magnetic field.

For mO ions, we have chosen the orientation proposed by Colomban *et al.* in which two hydrogen atoms lay in the conduction plane.[6] This orientation is favored by hydrogen bonding and this allows us to determine completely the position of a d-mO NH_4^+ tetrahedron once the direction of the displacement of the center of the ion is fixed as in the defect 3(a). This is shown in Fig. 6.

For BR ions, two different kinds of orientations have been proposed in the past. From the NMR study of the rotational tunneling at liquid helium temperature, Gourier and Sapoval (GS) deduced that these ions have a C_2 axis parallel to the crystal c axis.[8] From infrared and Raman studies, Colomban, Boilot, Kahn, and Lucazeau (CBKL) found that both BR and mO ions have two hydrogens in the conduction plane at room temperature.[6] Theoretical calculations by Bates *et al.* favor this last orientation.[7] For either of these orientations, the proton positions for each BR ion can be found by considering the crystal field symmetry. Since the center of the ion is shifted towards mO, the site has only one vertical plane of symmetry. This plane must also be a plane of symmetry for the NH_4^+ tetrahedra. In the GS case, the BR ions can have only two positions, equivalent by symmetry around the conduction plane and also equivalent for our calculations. In the CBKL case, there is only one position, which is favored by hydrogen bonding with the O(5) atoms. It is shown in Fig. 6.

We have recalculated the second moment M_S using sums (8) and (9) in the two cases. This correction needs in fact to be made only for first neighbors. The dmO–dmO contribution is found to increase by a factor of 1.45 while the dmO–BR contribution is lowered by a factor 0.75 for the CBKL orientation and by a factor of 0.84 for the GS orientation. The H–H contribution is found to decrease by 0.13 G^2 in the CBKL case and by 0.08 G^2 in the GS case. For the $^1H-^{27}Al$ contribution, we find decreases of 0.06 G^2 and 0.03 G^2, respectively.

The final theoretical values for M_S are 1.96 and 2.04 G^2 for the CBKL and GS orientation, respectively. For M_N, similar corrections give 1.35 and 1.43 G^2. For both orientations, the agreement between the second moments calculated for the defect 3(a) and the experimental second moments is excellent.

V. CONCLUSION

Two facts have been neglected which require comments. First, the ratio of the number of BR ions to the number of mO ions in defect 3(a) is larger than the aver age value corresponding to the composition $x=0.3$. In other words, it is not possible to construct a conduction plane compatible with our stoichiometry by a simple juxtaposition of defects 3(a). Defects must overlap, with some of the BR ions participating to two defects. This effect tends to increase the second moment. We have estimated that for M_S, this increase is of the order of 0.1 G^2. Secondly, the crystal is not perfectly exchanged. The 2% of remaining Na^+ ions probably occupy mO sites since they are smaller than NH_4^+ ions.[18] We have calculated that this would decrease M_S by about 0.05 G^2. Therefore, these two effects nearly compensate.

We can then conclude that the agreement between our calculation and the experiment is corroborating the ex-

istence of the defect 3(a) with displaced mO ions (by 1.1 Å from mO towards aBR) and displaced BR ions (by 0.13 Å towards mO as shown in Fig. 5). The overall agreement is slightly better when BR ions are taken in the CBKL orientation as shown in Fig. 6, but present results do not permit to eliminate the orientation proposed by Gourier and Sapoval.

We find it remarkable that such a detailed picture of a complex disordered medium can be discussed starting from a measure of the second moment of a NMR line.

ACKNOWLEDGMENTS

We are grateful to Dr. Jean-Pierre Boilot and Dr. Philippe Colomban for helpful discussions.

[1]A large number of references on the subject can be found in the proceedings of the last conferences on Fast Ion Transport held in Lake Geneva (1979), Tokyo (1980), and Gatlinburg (1981) and published respectively in: *Fast Ion Transport in Solids*, edited by P. Vashishta, J. N. Mundy, and G. K. Shenoy (North-Holland, Amsterdam, 1979); Solid State Ionics 3, 4, (1981); Solid State Ionics 5 (1981).
[2]D. Wolf, J. Phys. Chem. Solids 40, 757 (1979).
[3]W. L. Roth, F. Reidinger, and S. La Placa, in *Superionic Conductors*, edited by G. D. Mahan and W. L. Roth (Plenum, New York, 1976), p. 223.
[4]M. S. Whittingham and R. A. Huggins, J. Electrochem. Soc. 118, 1 (1971).
[5]J. C. Wang, N. Gaffari, and Sang-il Choi, J. Chem. Phys. 63, 772 (1975).
[6]Ph. Colomban, J. P. Boilot, A. Kahn, and G. Lucazeau, Nouv. J. Chim. 2, 21 (1978).
[7]J. B. Bates, T. Kaneda, J. C. Wang, and H. Engstrom, J. Chem. Phys. 73, 1503 (1980).
[8]D. Gourier and B. Sapoval, J. Phys. C 12, 3587 (1979).
[9]R. C. T. Slade, P. F. Fridd, T. K. Halstead, and P. McGeehin, J. Solid State Chem. 32, 87 (1980).
[10]A. R. Ochadlick Jr., H. S. Story, and G. C. Farrington, Solid State Ionics 3, 4, 79 (1981).
[11]For a review of the effects of molecular tunneling on NMR absorption, see M. M. Pintar in NMR *Basic Principles and Progress*, edited by M. M. Pintar (Springer, Berlin, 1976), Vol. 13, p. 125.
[12]H. Arribart, H. Carlos, and B. Sapoval (to be published).
[13]R. Bersohn and H. Gutowsky, J. Chem. Phys. 22, 651 (1954).
[14]G. Collin, Ph. Colomban, J. P. Boilot, and R. Comes, in *Fast Ion Transport in Solids*, edited by P. Vashishta, J. N. Mundy, and G. K. Shenoy (North-Holland, Amsterdam, 1979), p. 309.
[15]E. R. Andrew, Phys. Rev. 91, 425 (1953).
[16]J. Itoh, R. Kusaka, and Y. Saito, J. Phys. Soc. Jpn. 17, 463 (1962).
[17]A. Abragam, in *The Principles of Nuclear Magnetism* (Oxford University, Oxford, 1961).
[18]J. P. Boilot, Ph. Colomban, J. Théry, G. Collin, and R. Comés, J. Phys. (Paris) 39-C2, 204 (1978).